Sensors & Actuators: B. Chemical 343 (2021) 130085

Contents lists available at ScienceDirect

Sensors and Actuators: B. Chemical

journal homepage: www.elsevier.com/locate/snb

Thrombogenicity of microfluidic chip surface manipulation: Facile, one-step, none-protein technique for extreme wettability contrast micropatterning

Yi Xu [a], Pan Deng [a], Guang Yu [b], Xingxing Ke [a], Yongqing Lin [c], Xiaorong Shu [c], Yaping Xie [a], Shuo Zhang [a], Ruqiong Nie [c], Zhigang Wu [a,*]

[a] State Key Laboratory of Digital Manufacturing Equipment and Technology, School of Mechanical Science and Engineering, Huazhong University of Science and Technology, Wuhan, China
[b] Experimental Medicine Center, Tongji Hospital, Tongji Medical College, Huazhong University of Science and Technology, Wuhan, China
[c] Department of Cardiology, Sun Yat-Sen Memorial Hospital, Sun Yat-Sen University, Guangzhou, China

ARTICLE INFO

Keywords:
Thrombogenic surface patterning
Microfluidic chip
Micro-nanostructured surfaces
Wettability conversion
Platelet-surface interaction
Biosensors

ABSTRACT

Surface engineering of well-defined micro-nanoscale surface topographies on polymeric materials of microfluidic chip has been explored as a promising strategy for platelet function testing and clinical diagnostics. However, the current methodologies of constructing platelet-patterned surfaces require different bioactive ligands with laborious and complicated steps, and bioactive proteins are expensive and easy to deactivate. To address these issues, by selective exposure of the nanoparticles in a silica doped silicone and surface topography tuning via an ultraviolet laser, we introduced a simple, one-step, cost-effective strategy for tuning of different states of wetting characteristics simultaneously and serve as a thrombogenic polymer surface. Microscale in situ observations show that the specific micro-nano hierarchical structure and mechanism of extreme wettability conversion in turn trigger the platelet activation and aggregation. *In-vitro* investigations show that both the micro-topography and wettability of microchannel are important factors for fabricating blood compatible, or high thrombogenic materials. We expect such a simple, no-protein technique could serve as a low-cost platform for biomaterials and biosensors, and may lead to a new protein-free methodology for coagulation tests and clinical diagnosis.

1. Introduction

Platelets play an essential role not only in hemostasis and arterial thrombosis, but also in other physiological and pathophysiological processes [1,2]. During hemostasis, platelets are rapidly recruited and become highly adhesive to the site of injury on the vessel wall and then undergo a sequence of biological changes to form thrombus [3]. Similar processes may occur in arteries and veins, and eventually lead to myocardial infarction or stroke [4]. Therefore, platelet adhesion and further aggregation is a critical step to mediate related physiological and pathological processes.

Surface engineering of a material is known to influence biological processes including cell behaviors, blood-contacting properties and so on [5]. It has implications for materials applied for microfluidic devices, biosensors, and implant materials [6]. As microfluidics can mimic the atherosclerotic confinement of vessels, physiological shear rates and the structure of injured blood vessels, numerous studies have examined human whole blood using such technologies combined with extracellular matrix surface engineering [7–9]. The surface engineering in microfluidic devices is emerging as a novel and powerful tool to manipulate the thrombogenicity of materials in spatially confined areas for platelet function diagnosis and the assay of antiplatelet drugs. For example, Muthard et al. introduced a defined flow sensing mechanism to regulate clot function [10]. Alonso et al. reported a method to quantify platelet-protein interactions with microarray of contact printed fibrinogen dots [11]. Ye et al. patterned surfaces for controlling platelet adhesion via polymerization method [12]. Eichinger et al. studied the antiplatelet drug efficacy based on margination of platelets contacting with surface-immobilized agonists [13]. Jose et al. demonstrated that cell adhesion to protein matrices can be used as a diagnostic tool in cardiovascular diseases [14]. Until now, various methods to develop platelet-patterned surfaces by a combination of surface chemistry and

* Corresponding author.
E-mail address: zgwu@hust.edu.cn (Z. Wu).

https://doi.org/10.1016/j.snb.2021.130085
Received 10 December 2020; Received in revised form 20 April 2021; Accepted 6 May 2021
Available online 7 May 2021

micro/nanotechnology such as microcontact printing [15], photolithography [16], e-beam lithography [17]. As it is known that platelets can bind directly to injured blood vessel walls with a large number of macromolecules, such as laminin, fibronectin, collagen, and von Willebrand factor (vWF). Therefore, the widely used strategy is to introduce a pattern of platelet-adhesive bioactive agonists on the inert substrates that allow platelets to adhere onto the pattern [18].

Successful microfluidics assays applying elaborate patterning of bioactive agonists, such as fibrinogen [18,19], collagen [20], fibronectin [15], and vWF [21] have been extensively studied, and several have been successfully pursued to develop platelets-patterned surfaces. However, these approaches consist of multi-step chemical grafting treatments or polymerization technologies. They are generally time-consuming and complicated. What's more, bioactive proteins are often expensive, easily inactivated, and specific to different platelet receptors [22]. Often, a poor correlation is observed between the results from different activation pathways. Therefore, the clinicians need to know the detailed methodological difference for specific measurement of platelet function [23], and consequently lead to limited usage in the clinical practice. In contrast, without any external activation conditions (e.g. agonists), a physical method of non-protein platelet-pattern surfaces in microfluidic chips is preferable to transform such a technology into a standard technique in clinics for testing platelet function, thrombotic potential or bleeding risk. Inspired by shear gradient theory for platelet activation and aggregation [24,25], a blood flow changes in micro/nano structure might be achieved without extra agonists. Nature tissue surfaces such as blood vessels exhibiting micro/nano topography have been found to influence cell behaviors, i.e., morphology [26], adhesion [27] and motility [28] in static and flow conditions. Controlling micro-nano scale pattern in chemical and topographic substrate is of great help to develop purpose-specific cell-regulating cues in various biomedical applications [29], i.e., tissue engineering, implants, cell-based biosensors, microarrays, and basic cell biology. Biomimetic surfaces, i.e., superhydrophobic and superhydrophilic surfaces, with unique micro/nano structure have attracted extensive interest due to their great potential for fundamental and biomedical applications [30, 31]. However, to our knowledge, only a few studies on the potential biomedical applications of non-protein wettability contrast patterns in microfluidic chips for coagulation tests and diagnostics, have been reported [32]. Further, it is not clear to what extent fabricated surface topography and wettability influence platelet behavior and by what mechanism. Systematic studies are essential to understand the effects of micro-nano structure and extreme wettability contrast on platelet-polymer interaction in both static and hemodynamic conditions.

In this work, microfluidic chip fabrication and surface engineering are employed to mimic the local pathological environment experienced in living arterioles (Fig. 1A). To study platelet activation and adhesion on different wettability surfaces, we propose a simple method for controlling micro/nano scale pattern and their chemical and topographic attributes on silicone substrate (Fig. 1B, C). Merely by tuning a few laser operational parameters, the micro patterning surface can be simultaneously converted from hydrophobic to either superhydrophilic or superhydrophobic in a short time (Fig. 1D). Further, a flexible non-protein microfluidic platform was set up for further platelet adhesion and aggregation study (Fig. 1F). Such a platform is proved to be an

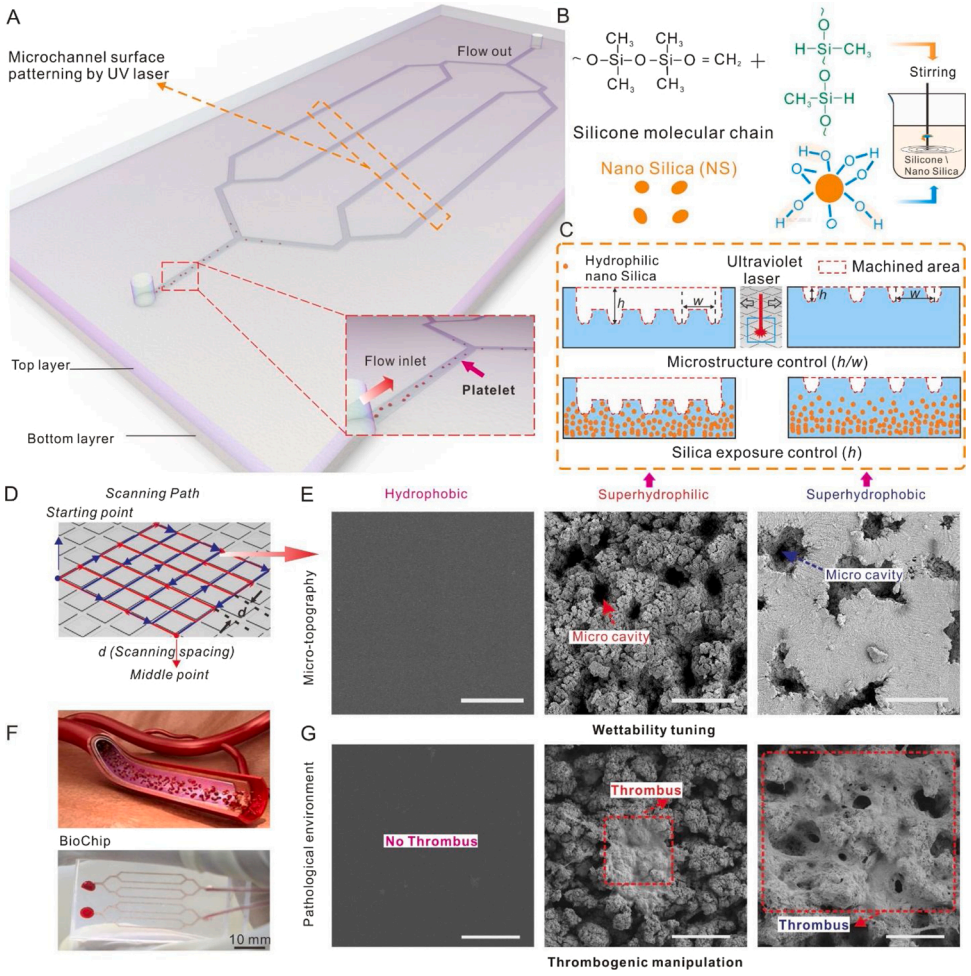

Fig. 1. Biomimetic microfluidic device for platelet activation and aggregation investigation. (A) Schematics of the platelet aggregation monitoring device and the method. (B) Preparation of PDMS-silica composite. (C) Schematic illustration of the mechanism of wettability conversion. (D) Schematic illustration of surface patterning by a UV laser scanning. (E) SEM images of three different wettability surface after UV laser treatment. Scale bar =50 μm. (F) Photograph of multi-channel bio-mimic hemostasis monitoring microfluidic device. (G) SEM images of blood clots formed inside the microfluidic chip. Scale bar =50 μm.

effective tool to study platelet polymer interaction in both static and flow conditions (Fig. 1E, G).

2. Materials and methods

2.1. Materials and reagents

A PDMS-silica nano composite was prepared by mixing commercial silicone elastomer (Sylgard 184, Dow Corning Corporation) with silica nanoparticles (Size: 7−40 nm, Sigma-Aldrich, China). The platelets were fluorescently labelled with Calcein-AM (Dojindo Laboratories, Shanghai, China) for platelet adhesion and aggregation microscopy. Glutaraldephyde (Ybio Tech, Shanghai, China) in Phosphate buffered saline (PBS) (BasalMedia, Shanghai, China) were used for platelets fixing and further scanning electron microscopy. PBS contains 137 mM NaCl, 2.7 mM KCl, 4.3 mM Na_2HPO_4, and 1.47 mM KH_2PO_4, with pH 7.4. All the chemicals are analytical grade and used without further treatment if not mentioned.

2.2. Micro-/nanostructure fabrication

The PDMS-silica piece was scanned by vertically crossed line by line via a UV laser marker (HGL-LSU3/5EI, Huagong Laser, Wuhan, China). Experiments revealed that the optimal results were achieved at a repetition frequency of 80 kHz, pulse width of 0.2 μs, working current of 33.5 A and scanning velocity of 150 mm/s in our laser system. The laser spot is about 20 μm. The laser scanning path is thematically shown in Fig. 1D. The scanning spacing between two adjacent lines ranged from 3 to 25 μm in both *x* and *y* direction.

2.3. Blood collection and platelet preparation

Whole human blood was drawn from medication-free healthy volunteers, who has no hematological relevant medical history. The blood was collected into the syringes containing sufficient heparin (the experiments were carried out in accordance with the guidelines issued by the Ethical Committee of Huazhong University of Science and Technology for NSFC project 31,400,929). The first few drops of blood were discarded to retain the platelets that were not activated. To prepare platelet-rich plasma (PRP), anti-coagulated blood was transferred from the syringe for the first spin (soft spin) at 130 g for 15 min.. The clouded phase was directly collected by gently aspirating with a pipette. To further concentrate PRP, a second 15-min spin (hard spin) was performed at 250 g for 15 min.. Then, pellets containing platelets were re-suspended. The PRP was stored at 4℃ and experimented within 4 h of collection. To reduce the blood volume for analysis, the PRP was diluted 10 times before it entered the microfluidic chip for further hemodynamic analysis.

2.4. Preparation of PDMS-silica composite

The PDMS-silica was made by mixing silicone base/curing agent 10:1, with fumed silica nanoparticles at a weight ratio of 9g:1 g by a Thinky® Mixer, USA. The mixture was firstly mixed by a bubble free mixer for 1 min and then dispersed and degassed for 1 min, separately. The procedure was repeated for twice. The preparation process is shown in Fig. S1.

2.5. Microchannel fabrication

The microchannel was fabricated by following a standard soft lithography. The microfluidic chips were designed to fit on a standard microscopy slide to facilitate microscopic analysis using AutoCAD (version 2018). Sylgard 184 PDMS was cast on the silanized master on Si wafers. The PDMS slab was cured at 75℃ in an oven (UF 55 plus, Memmert, Germany) for 30 min., then peeled off and treated by the UV laser. Finally, 2-mm holes were punched for inlets/outlets and bonded to another PDMS slide.

2.6. Principle of coagulation monitoring

The platelet sample in a 5-ml syringe was primed via a syringe pump (PHD2000, Harvard Apparatus, Boston, USA). Fluorescence images (recorded at 3-s time intervals over 150 s) and following intensity quantification were used to indicate the amount of adhesion and aggregation and analyzed using MATLAB image segmentation and a binary processing method (Fig. S2). Polythylene (PE) tubing was connected to the inlet and outlet of microfluidic chip. To study the interaction of microchannel surface and platelet adhesion with different wettability, pattern geometry and roughness, the surface was treated with the UV laser at different parameter settings. In the studies with PRP, various shear rates were applied to mimic the physiological and pathological environments. All studies were performed at a shear rate of 4000 and 8000 s^{-1} to determine the clotting time and analyze the response to different shear rates within a few mins. Thrombus formation was observed using a time-lapse imaging under a Nikon Ti-u, Tokyo, Japan, with fluorescently labelled platelets (Calcein-AM, Dojindo Laboratories, China).

2.7. Surface characterization

All the samples were completely vacuum dried prior to characterization. UV−vis absorption was conducted on a spectrophotometer (SolidSpec-3700, Japan). Static contact angles were measured at room temperature with 2−6 μl of water (Milli-Q) droplets using a drop shape analysis equipment (DSA25, KRUSS, Germany). Scanning electron microscopy (SEM) images were acquired on a GeminiSEM300 (Carl Zeiss, Germany). The samples were sputter coated with gold before imaging. The cross-section image was directly cut from the sample surface. The machining depth *h* and distance between cavities (*w*) can be both measured by the SEM attached program. Energy dispersive X-ray spectroscopy (EDS) profiles were acquired by using an Oxford X-Max EDS detector. The roughness and machining depth of the surface were analyzed using an ultra-depth three-dimensional microscope (DXS 510, Olympus, Japan).

2.8. Sample preparation of platelet-surface interaction for SEM imaging

It should be noted that the biochip is perfused with water to maintain the superhydrophilic microchannel surface in wet environment before the study of platelet-surface interaction, while the other two wettability surface channel are not necessary for the same procedure. In the static state analysis, the obtained PRP was carefully introduced on the surfaces of UV laser treated PDMS-silica composite film. In the hemodynamic state analysis, the PDMS to PDMS bonded microchips were peeled off manually after thrombus formation. The observation region of the chip was cut in ~1 × 1 cm sizes and washed three times in PBS with shaking to remove the loosely adhered cells and platelets. The platelets on both surfaces were fixed with 2.5 wt% glutaraldehyde in PBS solution for 4 h, and dehydrated in ascending grades of ethanol (50, 70, 80, 90, and 100 % (v/v) solution) for 15 min each. The films were dried at room temperature for 20 min, sputter coated with 5 nm gold and imaged on a GeminiSEM300 (Carl Zeiss, Germany). The platelet coverage on the film was quantified by counting the total number of adherent platelets from random SEM images at the same magnification under the static state. The morphology of adhered platelets with the shape of discoid, dendritic, spread was further classified.

2.9. Statistical analysis

All experiments were run in triplicate and repeated separately for at least three times. Data obtained from the different assays are presented

as mean values with standard deviations.

3. Results and discussion

3.1. Physico-chemical characterization of bi-philic surface

PDMS is widely used in microfluidics due to numerous advances in fabrication and biomedical applications. Of particular, it has a low surface energy, and can serve a good candidate for the preparation of hydrophobic surfaces. Manipulating its wetting characteristics, we are in pursuit of finding a none-protein containing technique for effective study of platelet-surface interaction.

As shown in Fig. 1B, after hydrophilic silica nanoparticles doped, PDMS-silica composite surface with microcavities were obtained by vertically crossed UV laser scanning (Fig. 1D) with scanning interspace d ranging from 3 to 25 μm. From the SEM images (Fig. 1E and Fig. S3), we observe that the average value of micro cavity arrays is distributed on the obtained superhydrophilic and superhydrophobic surface, respectively. On the superhydrophilic surface, numerous micro-nano cauliflower like structures are randomly distributed while rather smooth surface between the micro cavities are formed on a superhydrophobic surface (Fig. S3). The cross sections of the surface show that the machining depth h of the superhydrophilic surfaces is much deeper than the superhydrophobic ones (Fig. S3). It should be noted that there is no significant difference between the machined and unmachined surface only with ablation cavities of the superhydrophobic substrate compared with superhydrophilic one (Fig. S3 Cross Section). During the UV laser ablation, the depth h and distance between the cavities w are both tuned by varying the scanning spacing (SS), d (Fig. 1C). As the diameter of the cavities is almost the same and determined by the fixed laser spot. Notably, the machining depth h is highly related to the critical diameter of the laser spot L while the distance between cavities w is proportional to the SS. Hence, when the SS is chosen to be much smaller than L, the overlapping machining happens with deeper depth (h) and smaller distance (w) while the SS is slightly larger than L, there is no overlapping only with machining cavities of lower depth (h) and larger distance (w) (Fig. 1C).

To illustrate the formation mechanism of extreme wettability conversion, a schematic of the chemical conversion and structure formation are shown in Fig. 2A. The surface in a microfluidic chip was micro-patterned by the UV laser to produce regions with different wettability for further platelet adhesion tests, Fig. 2B. According to the Wenzel and Cassie model, roughness plays an important role in the wetting behaviors of solid surfaces and enhances their intrinsic wetting properties [33], though roughness alone will not change a surface from hydrophobic to both superhydrophobic and superhydrophilic simultaneously. In principle, both photon-chemical reaction and concentrated dense energy diffusion should be involved during the UV laser patterning. Hence, additional Si−OH (or similar hydrophilic group) will be generated by the photon-chemical reaction [34], Fig. 2C. While the accompanying thermal energy was overloaded and diffused into PDMS surface or blasted parts from the surface to the interior, which resulted of meso-/micro/nano-scale structure [35]. However, as obvious superhydrophilic intermediate state is not observed in the transition from hydrophobic to superhydrophobic surface. It indicates that few Si−OH was generated by the weak UV radiation effect, and meanwhile high contrast machining depth h indicates that concentrated dense energy dominates during our processing. Furthermore, based on the previous study [36], the doped particles are suspended in the PDMS precursors and will be precipitated over time before curing. Consequently, a thin layer of the particle concentration gradient will be formed from nearly zero to the final averaged concentration near the surface and memorialized after fully cured. Therefore, we hypothesize that hydrophilic nano silica exposure after UV laser ablation is a dominant factor to the wettability switching. The exposure is governed by the ablation depth (h) which caused by the UV laser (Fig. 2A, left panel). Moreover, the exposure number of hydrophilic silica nanoparticles on the surface and detailed topography are both correlated to the aspect ratio (h/w) which is depend on the SS (Fig. S4), and hence leads to totally different wetting behaviors.

Further, the SiO_2 particle exposure are investigated by a Fourier transform infrared spectroscopy (FTIR) and energy dispersive spectrometer (EDS) on three different wettability surfaces (Fig. S5 and Fig. S6). As shown in Fig. S5, after the UV laser treatment to create a superhydrophobic surface, the spectrum shows the same peaks as the pristine surface (black line) which indicate that no further Si-O-Si

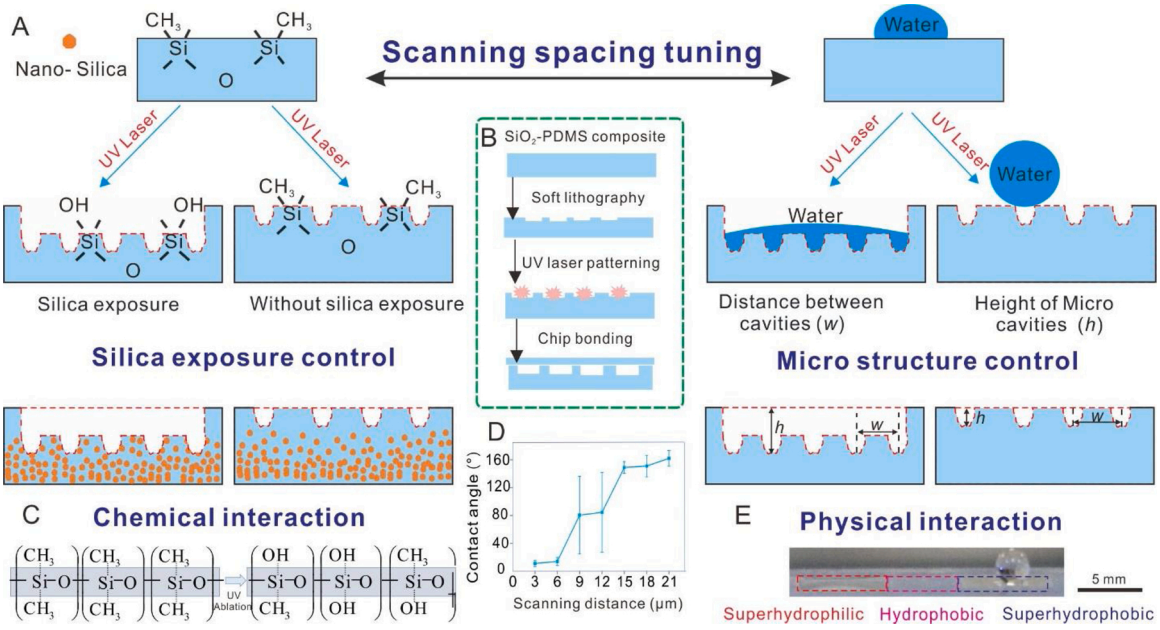

Fig. 2. The proposed strategy of wettability tuning via a UV-laser system. (A) Schematic illustration of chemical composition conversion and structure formation. (B) Schematic representation of the fabrication process of a microfluidic device with different wettability surfaces. (C) Chemical mechanism for conversion of functional groups on PDMS-silica surfaces by UV laser irradiation. (D) Water contact angles of PDMS-silica composite surface as a function of the distance (d) separating UV scanning lines. (E) A droplet of water on superhydrophobic and superhydrophilic surface.

generated. However, the spectrum of the superhydrophilic surface shows additional absorption peaks at 1085 and 1025 cm^{-1} associated with Si-O-Si stretch. Moreover, a broad band appears below 1000 cm^{-1} with no peaks at 750−865 cm^{-1} that indicate degradation of the Si−CH_3 bond (Fig. S4, red line). As shown in Fig. S6, after UV laser treatment for 30 s, the C peak decreased while the O peak increased compared with the pristine PDMS-silica surface. These results suggest that high density UV laser treatment brings additional Si-O-Si network structures on the superhydrophilic surface. Combining with the aforementioned finding on our laser features during the process, it further strengthens our hypothesis that the exposed hydrophilic silica nanoparticles play a significant role on improving its hydrophilicity. It also complies with our observation that the droplet quickly attaches onto the sample surface when it approaches superhydrophilic zone (left panels), meanwhile the droplet can barely attach to the superhydrophobic zone (right panels), Fig. S7, since the apparent contact angle is Cassie-Baxter angle and mainly depends on geometry of the cavities and pitch value (*w)* [37]. In addition, the light is scattered by the patterned micro-topography, resulting in a decreased optical transparency of the surfaces as shown by low transmission across the visible spectrum (Fig. S8).

In brief, with selectively silica nanoparticles exposure, the micro-topography and wetting characteristics can be controlled by SS during the laser process, where a series of chemical and physical interactions happen consequently. Therefore, precise tuning of the UV laser system, an extreme wettability conversion can be easily achieved in a single processing, Fig. 2E. Compared to other methods used for fabricating microstructures in microfluidic device [38–41], our approach has several advantages: Firstly, the UV laser micro patterning is a fast process, typically within 30 s; Secondly, the fabrication process can be controlled in a simple way. Thirdly; both microfluidic channel and surface modification can be integrated using a same UV laser [42]; More importantly, both superhydrophobic and superhydrophilic surfaces can be obtained by a one-step UV laser parameter tuning.

3.2. Microfluidic chip design for hemodynamic monitoring

We designed a microfluidic chip, containing microchannels that mimic arterioles with different wettability surfaces, to produce shear stress when the blood is perfused through the microchannel (Fig. 1A). This was achieved by allowing the blood to first flow into a single entrance (800 μm wide, 75 μm high) and then splitting the flow into 4 parallel channels (800 μm wide, 75 μm high) that converge again to a shared outlet (Fig. 1F). The 4-channel design increases the throughput of the experiment, while simultaneously maximizing the surface area exposed to the flowing blood and enabling parallel diagnosis of the adhesive function of platelets. The design can produce a shear rate range from 0 to 20,000 s^{-1} appropriate for most physiological and pathological conditions. We operated the microchip to maintain the flow rate within the range of 90−450 μl min^{-1}, leading to a maximum wall shear rate from ~2,000 to 10,000 s^{-1} in the uniform region. Finite element analysis of non-Newtonian blood flowing through the chip confirmed that under a given inlet flow velocity, the wall shear rate remains mostly uniform in the straight channels. The relationship between shear rates and flow rates in the microchannel can be obtained by the Poisson equation,

$$V = \frac{6Q}{a^2 b} \tag{1}$$

where V (s^{-1}) is the wall shear rate and Q (μl/s) is the flow rate. The dimensions a and b (mm) are the depth and width of micro channel, respectively. Platelet behavior under different wall shear rates can be achieved by varying the pump flow rate. Thus, platelet adhesion and aggregation can be investigated under wall shear rates from 2,000 to 10,000 s^{-1} that are typically found in the clinical practice [43], for example, in the patients with arteriosclerosis.

The profile and machined depth of microchannel surface are shown in Fig. 3A for superhydrophilic and superhydrophibic surfaces, respectively. The relation between the depth of the microchannel and UV laser scanning spacing (SS) is shown in Fig. 3B. As it can be seen, the ablation depth decreases with an increase in the distance between scanning lines. The superhydrophilic surface has the maximum average surface roughness (Ra, Fig. 3C) while the superhydrophobic surface has the maximum root mean square of a surface (RMS, Fig. 3D). The result shows that more micro/nano structures formed on superhydrophilic surface while profile height deviations are larger than that on superhydrophobic surface (Fig. 1E). Based on **Eq.** (1), the wall shear rate is related to the machining depth of the microchannel that is dependent on SS. These results indicate that the wettability and roughness/topography of the microchannel surface as well as the shear rate are all related with the SS. Based on these findings, once the interaction between platelets and material surface properties are established, the manipulation of anti-thrombotic or thrombogenic materials surface can be further engineered by tuning the UV laser operational parameters.

3.3. Platelet activation and adhesion test without flow

Several cell types have been found to respond differently to the surfaces with varied topography in a diversity of shapes, scales and symmetry [29,44]. Here, platelet adhesion and aggregation on different wettability substrates quantitatively analyzed and correlated with the SEM images of substrate topography (Fig. 4A, B). Un-activated platelets have a disc shape with diameters of 2−3 μm while activated platelets exhibit pseudopodial or spread dendritic shapes [45]. The state of activation of platelets can be divided into several stages according to various activation levels: (1) round or discoid with no pseudopodia present; (2) activated with a pseudopodial morphology; and (3) activated with a dendritic morphology [46]. As revealed by the SEM images, platelets adhered on the pristine PDMS-Silica composite substrate, a portion of the platelets were round or pseudopodial and the remaining were partially or fully spread with no erythrocytes present (Fig. 4A, left panel). In contrast, few (if any) single platelets adhered on superhydrophilic surface substrates while small amounts of filamentous mesh were observed on the top of the micro-valley caused by the ablation (Fig. 4A, middle panel). Large amounts of filamentous mesh were formed on the superhydrophobic surface as shown in (Fig. 4A, right panel). On the basis of the formation of the filamentous mesh, we deduced that the micro/nano structure of the topography was able to stimulate platelet as a biocatalytic function during the clotting process.

Different responses of platelets to substrates with varying topography was also assessed where surface chemistry was varied. As mentioned in Section 3.1, the topographies of superhydrophobic and superhydrophilic surfaces were similar in terms of diameters (~20 μm) of microcavities. However, the distance between the micro cavities (w) was much different with 25 and 50 μm in superhydrophilic and superhydrophobic surfaces, respectively (Fig. 1E). What's more, the area between the cavities are hierarchical micro-/nano- structures on superhydrophilic surface unlike the smoother surface on superhydrophobic one (Fig. 1E). This result suggests that cavities with a larger spacing (w) act to increase the surface contact area for enhanced platelet adherence/interactions by allowing adhesion to occur [17]. In addition, as discussed in Section 3.1, due to the nano silica exposure on the superhydrophilic surface, when the blood is infused into the microchannel, a silica-water interface is expected to be formed. According to the previous study [47], the silica/water interface is negatively charged. Meanwhile, platelets have also negative charges on their surfaces in the presence of sialic acid (Nacetyl-neuraminic acid) [48]. Thus, we speculate that one of the reasons for the suppressing platelet activation with few clots formed is due to the platelets repelled by the negatively charged superhydrophilic surface.

PRP droplets placed on the superhydrophobic area exhibit nearly spherical shapes while the droplets spread completely on the

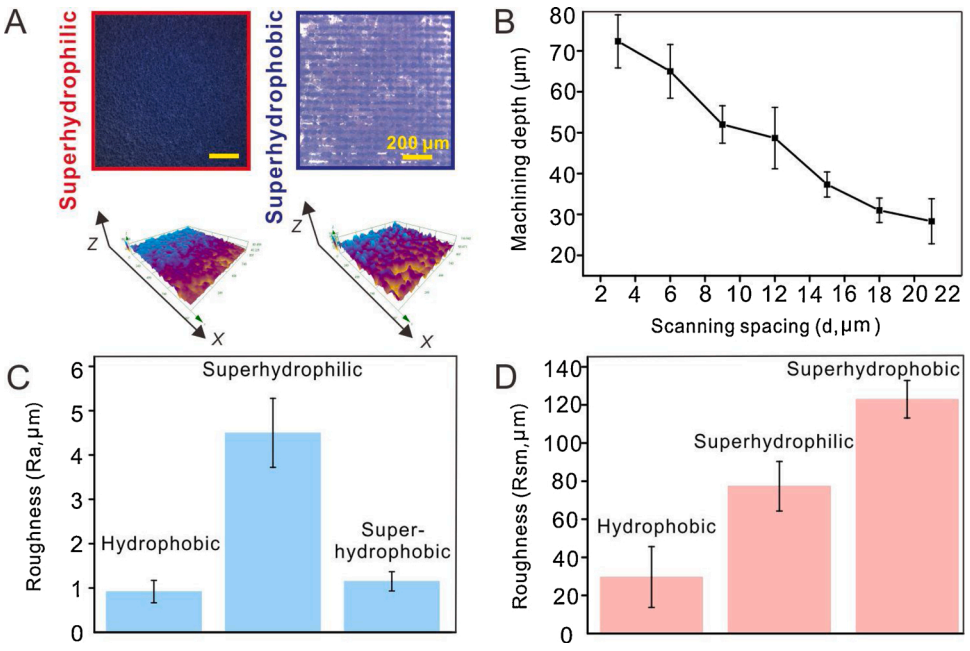

Fig. 3. Surface characterization of microfluidic chip channel. (A) Surface patterns and three-dimensional contours of the superhydrophilic and superhydrophobic surface treated by the UV laser. (B) Micro-channel depth as a function of distance between the UV laser scanning lines (C) Average roughness (Ra) of three typical wettability surfaces produced by the UV laser scanning. (D) Root mean square (RMS) roughness of three typical wettability surfaces produced by the UV laser scanning.

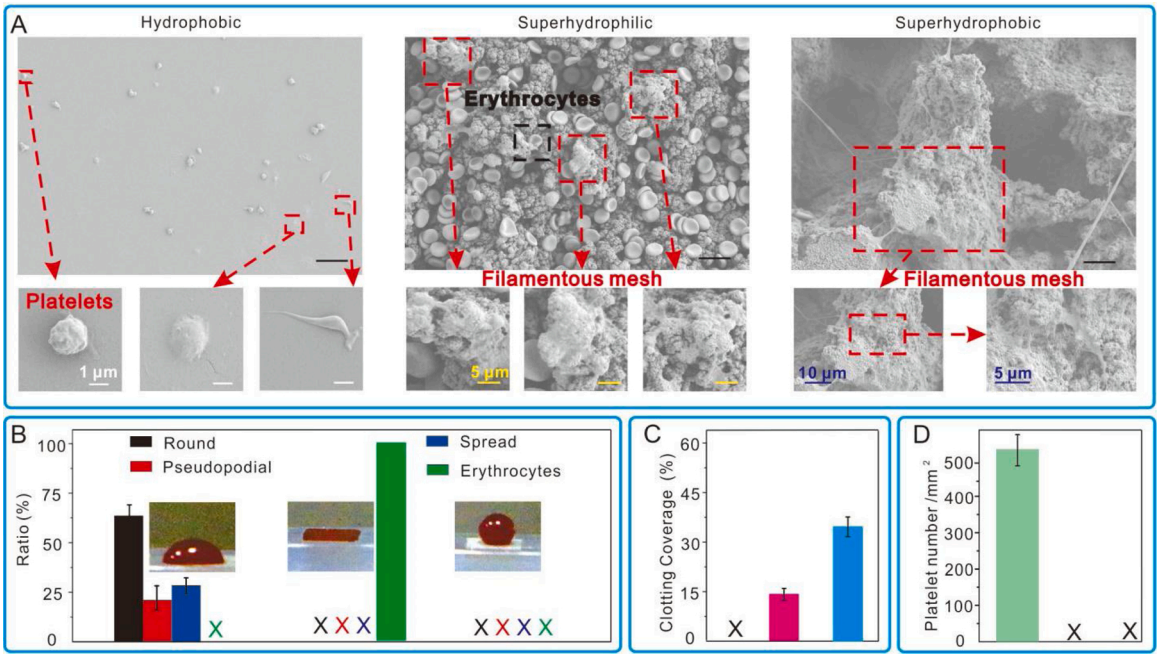

Fig. 4. Platelet activation and aggregation in static states. (A) SEM images of platelet adhesion and aggregation assays on three different wettability surfaces, scale bar =10 μm. (B) Quantitative analysis of the morphology of the adherent platelets and erythrocyte on three different wettability surfaces. (C) Clotting coverage on three different wettability surfaces. (D) Quantitative analysis of platelet number adhered on three different wettability surfaces. Three different wettability indicate hydrophobic, superhydrophilic and superhydrophobic from left to right in (B-D). The "×" indicates no platelets or erythrcytes.

superhydrophilic surface (Fig. 4B). It can be seen that the PRP droplets have the maximum contact area with the superhydrophilic surface (Fig. 4B, middle panel), while the contact area is minimum with the superhydrophobic surface (Fig. 4B, right panel). However, the area of clotting on superhydrophilic surface is much smaller than that on superhydrophobic surface (Fig. 4C). As seen in Fig. 4D, the single platelet morphology only exists on the smooth surface (hydrophobic) without clotting formation. All these observations indicate that micro topography and negative charges are the two important factors affecting the adhesion and aggregation of platelets. The role of these two factors in platelet activation and aggregation under hemodynamic conditions will be discussed in the next section.

3.4. In vitro investigation of platelet behavior under hemodynamic conditions

As platelet aggregation is a major cause of vascular occlusion [49] using microfluidics, thrombotic events can be studied on defined biopolymer surfaces under a constant flow rate. Platelet behaviors on three different wettability surfaces were imaged with fluorescence microscopy and SEM. Therefore, we explored whether the biochip described here can be employed as a biosensor to monitor platelet

adhesion and aggregation under pathological flow conditions.

As shown in Fig. 5A, few platelets (almost zero intensity) adhered to the pristine PDMS-Silica composite surface (hydrophobic domains). By contrast, a significant number of platelets adhered to the superhydrophobic domains (Fig. 5 C). With the superhydrophilic domains, a much smaller number of platelets can be adhered (Fig. 5B). The schematic configuration of the system is shown in Fig. S9. Platelet adhesion and aggregation on different wettability surfaces was recorded in Supplementary Video 1. The spacing between cavities (w) are different on three wettability surfaces as discussed in Section 3.3 demonstrating the role of this parameter in the platelet adhesion and aggregation.

The spacing between the cavities may influence the kinematic energy of the platelets. When the diluted PRP is perfused into the microfluidic chip, initially the velocity of the platelets will be the same as the flow velocity but the platelets will slow down as they pass through each cavity on the surface. Larger distances between cavities would allow the platelets to regain higher momentum. Thus, when the distances are longer, the kinematic energy of the platelet is higher. The shear rate is the change rate of velocity where platelet flow passes over the microchannel surface, therefore, the higher kinematic energy of the platelets obtained, the higher shear rate of the platelets experienced on the superhydrophobic surface, hence leading to more stable platelets aggregation (Fig. 1G, right panel). In general, the process of platelet activation to aggregation will be significantly influenced by kinematic energy loss. In combination with reactive thrombogenic surfaces, the degree of platelet aggregation is directly controlled by the magnitude and spatial distribution of shear gradients [24]. As discussed in Section 3.1, the silica-water interface is negatively charged. Therefore, the negatively charged platelets are repelled from the superhydrophilic surface and loosely adhered onto the surface. Therefore, those platelets are easily removed during the high shear rate and even on rougher surfaces little platelet aggregation occurs. However, the relative impact of micro-topography and negatively charged surface on the platelet aggregation is worth of further investigation.

Platelet aggregation is enhanced under hemodynamic compared to static conditions on both superhydrophilic and superhydrophobic surface, Fig. 5B, C. This can be explained by the fact that vWF is elongated into filaments binding 10–20 times at high shear stress as compared to static conditions [50]. Therefore, the vWF network can efficiently capture the moving platelets near the vessel wall to enhance of clotting behavior. By contrast, aggregation of platelet on hydrophobic surface is not enhanced under high shear rate where few single, activated platelets are observed (Fig. 5A) suggesting that, loosely adhered platelets are easily swept away by the high flow rate. Under high shear rate, only significant activated platelets form strong bonds to vWF so that subsequent aggregation can occur [51]. As shown in Fig. 6A, the results show that platelet coverage increases with the time on all three-different wettability surfaces. However, the thrombus coverage on the superhydrophobic surface is the highest indicating that this surface is highly thrombogenic; this suggests that such a surface will significantly promote thrombosis by regulating the rheological environment for platelet aggregation. All these results demonstrate that the platelet adhesion and aggregation have a strong correlation with the surface charges and micro topography that can be tuned by UV laser scanning parameters.

Usually, to reduce the blood volume and time required for analysis, the surface of the microchannel was functionalized with bioactive proteins, which is a common platelet agonist [52,53]. However, in our experiments, even without any agonists, we observed significant platelet aggregation on the superhydrophobic surface of the microchannel in a short time (~150 s, Fig. 5C). Thus, this microfluidic device is potential to be used for rapid platelet assays where less whole blood is required. The dynamics of platelet aggregation on superhydrophobic surfaces were investigated under both physiological and pathological conditions (Fig. 6B-D). Normally, wall shear rates >5000 s^{-1} are generally considered pathological [51]. Therefore, in our experiments, the shear rates were set to 4000 and 8000 s^{-1} to represent the physiological and pathological conditions, respectively. As it can be seen, thrombus grows much faster (Fig. 6B) and the thrombus coverage is much higher (Fig.6C) under pathological as compared to physiological conditions. The time to reach the same degree of thrombus coverage under pathological conditions is lower as compared to physiological conditions (Fig. 6D). In the current study, the results show a statistically difference of platelet aggregation between the shear rates on superhydrophobic surfaces, and demonstrate the important role of shear rate during the platelet adhesion and aggregation.

To study the stability and repeatability of microfluidic chip with superhydrophobic surface, the blood was collected from healthy volunteers and tested under an 8,000s^{-1} shear rate with different storage durations ranging from 1−4 hours. The results show that the average thrombus coverage is increased with the storage time decreases. The average thrombus coverage over different storage times is (47.5 ± 1.8)%, and the coefficient of variation (CV) is about 0.05,

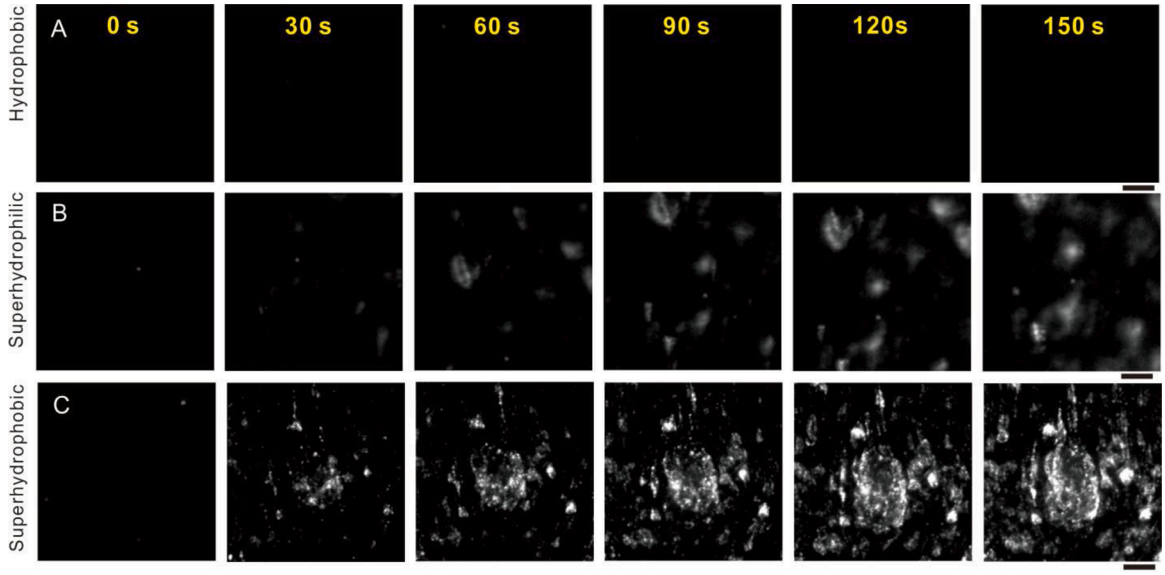

Fig. 5. Fluorescence microscopic images of thrombus formation with various surfaces under high shear. Scale bar =50 μm. (A) Hydrophobic surface. (B) Superhydrophilic surface (C) Superhydrophobic surface.

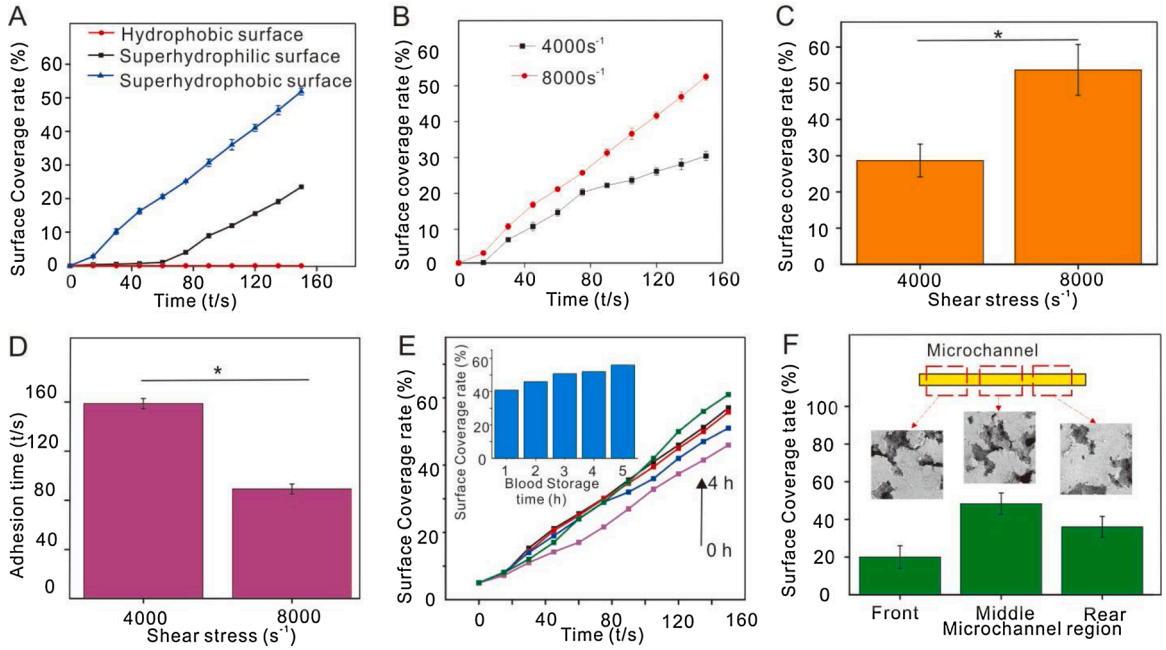

Fig. 6. Dynamic platelet aggregation in microfluidic chip. (A) Quantitative analysis of thrombus formation on a microfluidic chip as a function of time. (B) Quantitative analysis of thrombus formation under two different shear rates representing physiological and pathological conditions as a function of time. (C) Thrombus coverage at two different shear rates representing physiological and pathological conditions after 150 s. (D) Time to reach 28 % coverage at two different shear rates representing physiological and pathological conditions (E) Effect of blood (from the same volunteer) storage time on platelet adhesion and aggregation on a superhydrophobic surface. (F) Platelet coverage in three different regions in one microchannel with a superhydrophobic surface. Significance was tested by one-way ANOVA test, *: $p < 0.05$.

Fig. 5E. The thrombus coverage in the beginning, middle and rear regions of microchannel under the continuous flow of PRP from the same volunteer was investigated, Fig. 5F. The CV of platelet coverage is 0.08 after 150 s of flow in three different regions and the thrombus coverage is the highest in the middle of the microchannel. The phenomenon can be explained based on shear gradient theory as well [24]. It has been demonstrated that the microtopography of superhydrophobic surface will induce significant platelet aggregation. Therefore, the front position of the microchannel will form thrombus for the first time. Consequently, the thrombus formation will change the geometry locally and hence form stenosis site. According to the shear gradient theory, significant thrombus formation of platelet aggregates occurring in the downstream expansion zone. Therefore, the microtopography and following macro-stenosis will both enhance the thrombus formation in the middle region of the microchannel with the highest ratio of platelet coverage. In the rear region, the micro and macro effect also enhance the thrombus formation, however, the shear rate should be much lower than the middle region. Thus, the ratio of platelet coverage is lower than the middle and higher than the front region.

These experimental results clearly indicate that the microfluidic chip with UV laser treated surfaces can act as a biosensor to monitor thrombus formation and platform to manipulate the surface thrombogenicity for a selection of biocompatible or high thrombogenic materials in tissue engineering and so on. Development of a facile, none protein method with different wettability surface facilitate the construction of platelet-pattern surface matrix in a microfluidic chip, i.e., adhesion in certain portions of a surface while keeping other regions free of platelets for further anticoagulation dose monitoring [12,14].

4. Conclusions

In brief, we demonstrated that micropatterned surfaces can serve simply as an extracellular physical milieu without involving biomolecules to regulate platelet adhesion and aggregation. The tuning of aspect ratio h/w convert initially hydrophobic surface to either superhydrohilic or superhydrophobic simultaneously. The results of our investigation indicate that microstructured polymer surfaces with larger spacing between cavities (w) and no negative charges enhance platelet adhesion and subsequent aggregation especially under high shear rates. On the basis of the investigations, a facile, protein-free and low-cost micropatterning is readily fabricated. The methodology is potential to be applied as a flexible platform to study the interaction of blood cells with a large number of polymers and surfaces for the application of tissue engineering and biosensors. Interestingly, our superhydrophobic surface can initiate significant platelet aggregation in a short time without introducing any agonists, suggesting that it could be used to assess blood coagulation by validation of meaningful diagnostic information, i.e., measurement of fluorescent area, intensity, clot retraction force and antiplatelet essays, for future point-of-care coagulation monitoring.

CRediT authorship contribution statement

Yi Xu, Zhigang Wu and Ruqiong Nie: conceived the idea and supported the whole work. **Yi Xu:** designed the experiment and wrote the manuscript. **Yi Xu, Pan Deng, Xingxing Ke, and Guang Yu:** carried out the experiments. **Yi Xu, Yongqing Lin, Xiaorong Shu, Ruqiong Nie, and Zhigang Wu:** contributed to data discussion. **Zhigang Wu, Ruqiong Nie, and Yi Xu:** directed the project. All authors commented on the manuscript.

Declaration of Competing Interest

The authors report no declarations of interest.

Acknowledgements

The authors acknowledge the National Natural Science Foundation of China (Nos. 31400929 and 51575216) and Guangzhou Science and Technology Plan Project (Livelihood Science and Technology) (No.

201903010009) and China Postdoctoral Science Foundation Funded Project (No. 2020M672332) and Advanced programs of Hubei human resources and technology (No. 016100200).

Appendix A. Supplementary data

Supplementary material related to this article can be found, in the online version, at doi:https://doi.org/10.1016/j.snb.2021.130085.

References

[1] J.N. George, Platelets, Lancet 355 (2000) 1531–1539.
[2] E.J. Paola, V.D. Meijiden, J.W.M. Heemskerk, Platelet biology and functions: new concepts and clinical perspectives, Nat. Rev. Cardiol. 16 (2019) 166–179.
[3] D.D. Wagner, P.C. Burger, Platelets in inflammation and thrombosis, Arterioscler. Thromb. Vasc. Biol. 23 (2003) 2131–2137.
[4] V. Fuster, L. Badimon, J.J. Badimon, J.H. Chesebro, The pathogenesis of coronary artery disease and the acute coronary syndromes, New England J. Med. Surg. Collat. Branches Sci. 236 (1992) 242–250.
[5] S.A. Skoog, G. Kumar, R.J. Narayan, P.L. Goering, Biological response to immobilized microscale and nanoscale surface topographies, Pharmacol. Ther. 182 (2018) 33–55.
[6] E. Luong-Van, I. Rodriguez, H.Y. Low, N. Elmouelhi, B. Lowenhaupt, S. Natarajan, C.T. Lim, R. Prajapati, M. Vyakarnam, K. Cooper, Review: micro- and nanostructured surface engineering for biomedical applications, J. Mater. Res. 28 (2013) 165–174.
[7] K.B. Neeves, A.A. Onasoga, A.R. Wufsus, The use of microfluidics in hemostasis: Clinical diagnostics and biomimetic models of, vascular injury, Curr. Opin. Hematol. 20 (2013) 417–423.
[8] B.R. Branchford, C.J. Ng, K.B. Neeves, J.D. Paola, Microfluidic technology as an emerging clinical tool to evaluate thrombosis and, hemostasis, Thromb. Res. 136 (2015) 13–19.
[9] S.M. Hastings, M.T. Griffin, D.N. Ku, Hemodynamic studies of platelet thrombosis using microfluidics, Platelets. 28 (2017) 427–433.
[10] R.W. Muthard, S.L. Diamond, Blood clots are rapidly assembled hemodynamic sensors: Flow arrest triggers, intraluminal thrombus contraction, Arterioscler. Thromb. Vasc. Biol. 32 (2013) 2938–2945.
[11] A.L. Alonso, B. Jose, M. Somers, K. Egan, D.P. Foley, A.J. Ricco, S. Ramstrom, L. B. Desmonts, D. Kenny, Individual Platelet Adhesion Assay: Measuring Platelet Function and Antiplatelet, therapies in Whole Blood via Digital Quantification of Cell Adhesion, Anal. Chem. 85 (2013) 6497–6504.
[12] W. Ye, Q. Shi, S.C. Wong, J.W. Hou, H.C. Shi, J.H. Yin, Patterning surfaces for controlled platelet adhesion and detection of dysfunctional platelets, Macromol. Biosci. 13 (2013) 676–681.
[13] C.D. Echiger, A.L. Fogelson, V. Hlady, Functional Assay of Antiplatelet Drugs Based on Margination of platelets inflowing, Blood, Biointerphases. 11 (2016), 029805.
[14] B. Jose, P. McCluskey, N. Gilmartin, M. Somers, D. Kenny, A.J. Ricco, N.J. Kent, L. B. Desmonts, Self-powered microfluidic device for rapid assay of antiplatelet drugs, Langmuir. 32 (2016) 2820–2828.
[15] F.M. Zhang, G.C. Li, P. Yang, W. Qin, C.H. Li, N. Huang, Fabrication of Biomolecule-PEG Micropattern on Titanium Surface and Its Effects on, Platelet Adhesion, Colloids Sur B Biointerfaces. 102 (2013) 457–465.
[16] M.C. Howland, A.R. Sapuri-Butti, S.S. Dixit, A.M. Dattelbaum, A.P. Shreve, A. N. Parikh, Phospholipid morphologies on photochemically patterned silane monolayers, J. Am. Chem. Soc. 127 (2005) 6752–6765.
[17] L.B. Koh, I. Rodriguez, S.S. Venkatraman, The effect of topography of polymer surfaces on platelet adhesion, Biomaterials. 31 (2010) 1533–1545.
[18] L.E. Corum, C.D. Echinger, T.W. Hsiao, V. Hlady, Using microcontact printing of fibrinogen to control surface- induced platelet, adhesion and activation, Langmuir. 27 (2011) 8316–8322.
[19] T. Ekblad, L. Faxalv, O. Andersson, N. Wallmark, A. Larsson, T.L. Lindahl, B. Liedberg, Patterned hydrogels for controlled platelet adhesion from whole blood and plasma, Adv. Funct. Mater. 20 (2010) 2396–2403.
[20] K.B. Neeves, S.F. Maloney, K.P. Fong, A.A. Schmaier, M.L. Kahn, L.F. Brass, S. L. Diamond, Microfluidic focal thrombosis model for measuring murine platelet deposition and stability: PAR4 signaling enhances shear-resistance of platelet aggregates, J. Thromb. Haemost. 6 (2008) 2193–2201.
[21] M. Lehmann, K. Ashworth, M.M. Johnson, J.D. Paola, K.B. Neeves, C.J. Ng, Evaluation of a microfluidic flow assay to screen for von Willebrand disease and low, von Willebrand factor levels, J. Thromb. Haemost. 16 (2018) 104–115.
[22] J.D. McFadyen, M. Schaff, K. Peter, Current and future antiplatelet therapies: emphasis on preserving haemostasis, Nat. Rev. Cardiol. 15 (2018) 181–191.
[23] M. Lordkipanidze, Platelet function tests, Semin. Thromb. Hemost. 42 (2016) 258–267.
[24] W.S. Nesbitt, E. Westein, F.J.T. Lopez, E. Tolouei, A. Mitchell, J. Fu, J. Carberry, A. Fouras, S.P. Jackson, A shear gradient-dependent platelet aggregation mechanism drives thrombus formation, Nat. Med. 15 (2009) 665–673.
[25] A. Jain, A. Graveline, A. Waterhouse, A. Vernet, R. Flaumenhaft, D.E. Ingber, A shear gradient-activated microfluidic device for automated monitoring of whole, blood haemostasis and platelet function, Nat. Commun. 6 (2016) 10176.
[26] M.J. Dalby, M.O. Riehle, H. Johnstone, S. Affrossman, A.S.G. Curtis, In vitro reaction of endothelial cells to polymer demixed nanotopography, Biomaterials. 23 (2002) 2945–2954.
[27] R. Ravichandran, S. Liao, C.C. Ng, C.K. Chan, M. Raghunath, S. Ramakrishna, Effects of nanotopography on stem cell phenotypes, World J. Stem Cells 1 (2009) 55–56.
[28] S. Nasrollahi, S. Banerjee, B. Qayum, P. Banerjee, A. Pathak, Nanoscale matrix topography influences microscale cell motility through adhesions, actin organization, and cell shape, ACS Biomater. Sci. Eng. 3 (2017) 2980–2986.
[29] J.Y. Lim, H.J. Donahue, Cell sensing and response to Micro- and nanostructured surfaces produced by chemical and topographic patterning, Tissue Eng. 13 (2007) 1879–1891.
[30] E.J. Falde, S.T. Yohe, Y.L. Colson, M.W. Grinstaff, Superhydrophobic materials for biomedical applications, Biomaterials. 104 (2016) 87–103.
[31] T.A. Otitoju, A.L. Ahmad, B.S. Ooi, Superhydrophilic (superwetting) surfaces: A review on fabrication and application, J Ind Eng Chem. 47 (2017) 19–40.
[32] H. Lee, W. Na, B.K. Lee, C.S. Lim, S. Shin, Recent advances in microfluidic platelet function assays: moving microfluidics into., clinical applications, Clin. Hemorheol. Microcirc. 71 (2019) 249–266.
[33] T. Koishi, K. Yasuoka, S. Fujikawa, T. Ebisuzaki, X.C. Zeng, Coexistence and transition between Cassie and Wenzel state on pillared hydrophobic surface, Proc. Natl. Acad. Sci. U. S. A. 106 (2009) 8435–8440.
[34] C.M. Atayde, L. Doi, Highly stable hydrophilic surfaces of PDMS thin layer obtained by UV radiation and, oxygen plasma treatments, Curr. Topics Solid State Phys. 7 (2009) 189–192.
[35] S. Zhang, Q. Jiang, Y. Xu, C.F. Guo, Z. Wu, Facile Fabrication of Self-Similar Hierarchical Micro-Nano structures for Multifunctional Surfaces via Solvent-Assisted UV-Lasering, Micromachines. 11 (2020) 682.
[36] S. Selimovic, S.M. Maynard, Y. Hu, Aging effects of precipitated silica in poly (dimethylsiloxane), J. Rheol. (N Y N Y) 51 (2007) 325–327.
[37] M. Kanungo, S. Mettu, K.Y. Law, S. Daniel, Effect of Roughness Geometry on Wetting and Dewetting of Rough PDMS Surfaces, Langmuir. 30 (2014) 7358–7368.
[38] M.B. Esch, S. Kapur, G. Irizarry, V. Genova, Influence of master fabrication techniques on the characteristics of embossed, microfluidic channels, Lab Chip 3 (2003) 121–127.
[39] J. Husny, H.Y. Jin, E.C. Harvey, J.C. White, The creation of drops in T-shaped microfluidic devices with the 'modified' laser LIGA, technique: I. Fabrication, Smart Mater. Struct. 15 (2006) 117–123.
[40] K. Stephan, P. Pittet, L. Kleimann, P. Morin, N. Ouaini, R. Ferrigno, Fast prototyping using a dry film photoresist: microfabrication of soft-lithography, masters for microfluidic structures, J. Micromech. Microeng. 17 (2007) N96.
[41] Y. Xu, B. Jiang, Machining performance enhancement of deep micro drilling using electrochemical discharge machining under magnetohydrodynamic effect, Int. J. Adv. Manuf. Technol 113 (2021) 883–892.
[42] Z. Liu, W. Xu, Z. Hou, Z. Wu, Rapid prototyping technique for microfluidics with high robustness and flexibility, Micromachines. 7 (2016) 201.
[43] T.V. Colace, G.W. Tormoen, O.J.T. Mccarty, S.L. Diamond, Microfluidics and coagulation biology, Annu. Rev. Biomed. Eng. 15 (2013) 283–303.
[44] R.G. Flemming, C.J. Murphy, G.A. Abrams, S.L. Goodman, P.F. Nealey, Effects of synthetic micro- and nano-structured surfaces on cell behavior, Biomaterials. 20 (1999) 573–588.
[45] S.L. Goodman, Platelet-material interactions with model cardiovascular biomaterials, J. Biomed. Mater. Res. 45 (1999) 240–250.
[46] D.R. Myers, Y. Qiu, M.E. Fay, M. Tennenbaum, D. Chester, J. Cuadrado, Y. Sakurai, J. Baek, R. Tran, J.C. Ciciliano, B. Ahn, R.G. Mannino, S.T. Bunting, C. Bennett, M. Briones, A.F. Nieves, M.L. Smith, A.C. Brown, T. Suchek, W.A. Lam, Single-platelet nanomechanics measured by high-throughput cytometry, Nat. Mater. 16 (2017) 230–235.
[47] P. Leory, N. Devau, A. Revil, M. Bizi, Influence of surface conductivity on the apparent zeta potential of amorphous silica, nanoparticles, J. Colloid Interface Sci. 410 (2013) 81–93.
[48] V. Karagkiozaki, S. Logothetidis, S. Lousinian, G. Giannoglou, Impact of surface electric properties of carbon-based thin films on platelets activation, for nano-medical and nano-sensing applications, Int. J. Nanomedicine 3 (2008) 461–469.
[49] S.P. Jackson, The growing complexity of platelet aggregation, Blood. 109 (2007) 5087–5095.
[50] C. Siedecki, B. Lestini, K.K. Marchant, S. Eppell, D. Wilson, R. Marchant, Shear-dependent changes in the three-dimensional structure of human von Willebrand factor, Blood. 88 (1996) 2939–2950.
[51] D.C. Lauren, M. Casa, H.D. David, N.K. David, Role of high shear rate in thrombosis, J. Vasc. Surg. 61 (2015) 1068–1080.
[52] Y. Zheng, J. Chen, M. Craven, N.W. Choi, S. Totorica, A.S. Diaz, In vitro microvessels for the study of angiogenesis and thrombosis, Proc. Natl. Acad. Sci. U. S.A. 109 (2012) 9342–9347.
[53] R.M. Schoeman, K. Rana, N. Danes, M. Lehmann, J.A.D. Paola, A.L. Fogelson, K. Leiermann, K.B. Neeves, A microfluidic model of hemostasis sensitive to platelet function and coagulation, Cell. Mol. Bioeng. 10 (2017) 3–15.

Yi Xu received his M.Sc. Eng. in mechanical engineering from Duisburg-Essen University, Germany, in 2011, and then he worked as an assistant researcher on the Multibody system dynamics and control in the National Engineering Research Center, China, from 2011 to 2015. After that he received a joint Ph.D from University of Michigan, Ann Arbor, USA, and Huazhong University of Science and Technology (HUST), China, in 2018. He is currently working in the Intelligent soft materials lab (HUST) as a Postdoctoral Research Fellow. His research interests include Lab-on-a-chip systems and micro-machines for bio/medical applications.

Zhigang Wu is a distiguished professor at Huazhong University of Science and Technology (HUST), China. Before joining HUST, Dr. Wu was an associate professor in Microsystems Technology, Uppsala University, Sweden. The mission of Wu's research is to develop new fabrication and manufacturing technologies for liquid fused soft intelligent systems that can potentially bring new solutions for societal challenges. Currently, his research focus on technology and application development of 1) microfluidics for *in vivo* diagnosis, 2) liquid alloy based soft electronics, 3) intelligent soft robot. Dr. Wu was selected as in junior researcher program by Swedish research council in 2010 and Chutian Scholar by Hubei government in 2012. Dr. Wu is the founding executive chair of International Symposium of Flexible and Stretchable Electronics and the chair of conference of Soft Robot Theory and Technology, 2019, Wuhan. He is also sitting the editorial board of *J. Micromech. Microeng.*, *Micromachines* and guest editor of *Material Today Physics*.